Dynamics around solutes and solute–solvent complexes in mixed solvents

Kyungwon Kwak, Sungnam Park, and M. D. Fayer†

Department of Chemistry, Stanford University, Stanford CA 94305

Edited by Robin M. Hochstrasser, University of Pennsylvania, Philadelphia, PA, and approved May 18, 2007 (received for review February 23, 2007)

Ultrafast 2D-IR vibrational echo experiments, IR pump-probe experiments, and FT-IR spectroscopy of the hydroxyl stretch of phenol-OD in three solvents, CCl_4, mesitylene (1, 3, 5 trimethylbenzene), and the mixed solvent of mesitylene and CCl_4 (0.83 mole fraction CCl_4), are used to study solute-solvent dynamics via observation of spectral diffusion. Phenol forms a complex with Mesitylene. In the mesitylene solution, there is only complexed phenol; in the CCl_4 solution, there is only uncomplexed phenol; and in the mixed solvent, both phenol species are present. Dynamics of the free phenol in CCl_4 or the mixed solvent are very similar, and dynamics of the complex in mesitylene and in the mixed solvent are very similar. However, there are differences in the slowest time scale dynamics between the pure solvents and the mixed solvents. The mixed solvent produces slower dynamics that are attributed to first solvent shell solvent composition variations. The composition variations require a longer time to randomize than is required in the pure solvents, where only density variations occur. The experimental results and recent MD simulations indicate that the solvent structure around the solute may be different from the mixed solvent's mole fraction.

preferential solvation | solute–solvent dynamics | ultrafast infrared

Solvent mixtures (mixed solvents) play important roles in chemical industries and in research laboratories. The value of mixed solvents comes about, for example, through the enhancement of chemical reactivity by increasing reactant solubility or product separation (1). The physicochemical properties of solvent mixtures often show large deviations from the ideal behavior expected from Raoult's law.

Fast dynamics of mixed solvents about a solute have been explored using fluorescence and Raman echo spectroscopies. Maroncelli and coworkers used fluorescence Stokes shifts to measure solvation dynamics of coumarin in various mole fractions of binary solvents (2). They observed Stokes shift dynamics, which varied with the mole fraction of the mixture that were intermediate between those observed in the two pure solvents. The results were discussed in terms of the diffusive behavior of the solvent with no suggestion of preferential solvation of the solute.

Investigations of mixed solvent properties have shown that the solvent structure of the first solvation shell of a solute can be different from that found in the bulk solution (3, 4). Spectroscopic studies of preferential solvation have mainly studied ionic or dipolar probes (5). Recently, preferential solvation involving neutral organic molecules was investigated by using ^{1}H NOESY measurements (6). Many experimental studies have concentrated on the static properties of preferential solvation, for example, determining the solvent composition in the first solvation shell of a solute. Berg *et al*. (7) showed that appreciable inhomogeneity was present in a mixed solvent system using Raman echo experiments. The inhomogeneity was attributed to the composition variation in the first solvent shell of the solute. The results did not indicate preferential solvation.

Here we present a study of the solute phenol in the mixed solvent of mesitylene (1,3,5-trimethylbenzene) and CCl_4 and in the pure mesitylene and CCl_4 solvents using ultrafast 2D-IR vibrational echo spectroscopy. Phenol forms T-shaped hydrogen bonded complexes with substituted benzenes including mesitylene (4, 8–10). In the mixed solvents of substituted benzenes and CCl_4, the phenol complex and free phenol are in thermal equilibrium. By adjusting the ratio of the benzene derivative and the CCl_4, the equilibrium can be tuned so that both species (complexed and free phenol) have approximately the same concentration. This is manifested in the IR absorption spectrum of the phenol hydroxyl stretch, which displays two peaks of approximately equal amplitudes (8, 10).

Complexes are constantly dissociating and forming. The chemical exchange between the free and complexed forms of phenol has been directly observed by using vibrational echo chemical exchange spectroscopy (8, 10). The chemical exchange manifests itself in the 2D vibrational echo spectrum as the growth of off-diagonal peaks as T_w, the time between the second and third pulses in the vibrational echo pulse sequence, is increased (8, 11). Depending on the chemical makeup of the complex, the chemical exchange time (inverse of the complex dissociation rate constant) ranges from a few picoseconds to a few tens of picoseconds. For example, the phenol-bromobenzene complex dissociates in 6 ps, whereas phenol-mesitylene dissociates in 31 ps (10). The dissociation time has been directly related to the formation enthalpy of the complex (8, 10).

The phenol-mesitylene system was selected for this study because the time scales for spectral diffusion, that is, solvent structural fluctuations aside from chemical exchange, range from subpicosecond to ≈10 ps. For the phenol-mesitylene system, the spectral diffusion of both the complex and the free species in the mixed solvent can be studied without having to sort out complications arising from chemical exchange because the exchange is relatively slow compared with the other processes. Therefore, the spectral diffusion of the complex and of the free species can be studied in the same mixed solvent. In addition, phenol is studied in pure mesitylene (complex only) and in pure CCl_4 (free phenol only).

The results presented below show that the solvent structural dynamics manifested as the 2D spectral line shape as a function of T_w in the 2D-IR vibrational echo experiments divide into two time scales, an ultrafast component (subpicosecond) and a slower component (≈10 ps). The ultrafast component for free phenol is the same whether it is in the mixed solvent or pure CCl_4. The ultrafast component of the complex is the same whether it is in the mixed solvent or pure mesitylene. However, the slower components of the free phenol and complexed phenol depend on whether the species are in a pure solvent or the mixed solvent. These results, combined with IR pump-probe measurements of the vibrational lifetimes and orientational relaxation

Author contributions: M.D.F. designed research; K.K., S.P., and M.D.F. performed research; K.K. and M.D.F. analyzed data; and K.K. and M.D.F. wrote the paper.

The authors declare no conflict of interest.

This article is a PNAS Direct Submission.

Abbreviation: FFCF, frequency–frequency correlation function.

†To whom correspondence should be addressed. E-mail: fayer@stanford.edu.

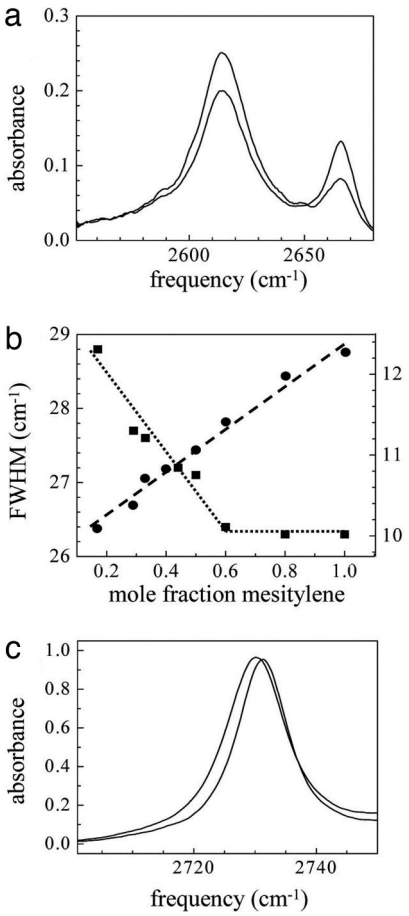

Fig. 1. Linear spectroscopy. (*a*) Spectra of the OD stretch of phenol-OD in the mixed solvent mesitylene/CCl_4 at two mole fractions. Lower frequency peak: T-shaped phenol-mesitylene complex. Higher frequency peak: free phenol (uncomplexed). The spectrum with the larger amplitude lower frequency peak has a mesitylene mole faction (χ) of 0.44, and the other spectrum has χ = 0.17. (*b*) Line widths as a function of mole fraction for the phenol-mesitylene complex OD stretch (squares, left axis) and a mesitylene band in the mixed solvent without phenol (circles, right axis). The line through the squares is an aid to the eye. The line through the circles is the best linear fit. (*c*) The mesitylene band in the mixed solvent at two mole fractions. The lower frequency peak is for a mesitylene mole fraction of 1 and the higher frequency peak is for a mole fraction of 0.17. Note that the shift in peak position is $\approx$1 cm^{-1}.

rates, are discussed in term of diffusive composition fluctuations in the first solvent shell. In addition, IR absorption experiments, some aspects of the 2D-IR data, and ideas from recent MD simulations (4) suggest that there is preferential solvation in the mixed solvent.

Results and Discussion

Linear Spectroscopy. The solvent background subtracted linear absorption spectra of phenol-OD in mesitylene/CCl_4 with various mole fractions (χ) of these two solvents were measured. Two of the spectra are presented in Fig. 1*a*. The peak at 2,614 cm^{-1} corresponds to the OD stretch of the hydrogen bonded T-shaped complex, phenol-mesitylene. The peak at 2,666 cm^{-1} is the OD stretch of free phenol. The sizes of the peaks vary as the equilibrium concentration of the two species is shifted by changing the mesitylene concentration. Because the bands overlap and change relative amplitude with changing mole fraction, it is difficult to determine whether there are small shifts in the peak positions (see below).

There is a measurable change in the line widths with mole fraction. The mole fraction of mesitylene was varied from 0 (pure CCl_4) to 1 (pure mesitylene). Fig. 1*b* shows the line widths of the phenol-mesitylene complex peak (squares, left axis) as a function of χ. The dotted line is an aid to the eye. The line width decreases with increasing mesitylene concentration, and the line width becomes independent of the χ for $\chi \geq 0.6$. The corresponding line width data for free phenol in the mixed solvent (not shown) displays the analogous trend. For small χ, the free phenol line width is χ independent and does not broaden until χ is large. If the line widths are mainly determined by the properties of the first solvation shell, these results suggests that the complex and free phenol are preferentially solvated by mesitylene and CCl_4, respectively.

Although the line widths change as a function of χ, within experimental error, the peak positions do not change. To examine this further, we took IR absorption spectra of 2-methoxyphenol-OD (2MP) in pure CCl_4 and in pure mesitylene. 2MP has an intramolecular hydrogen bond between the hydroxyl and the methoxy oxygen. It does not from complexes with mesitylene as evidenced by a single sharp peak in the spectrum at all χ. In going from χ = 1 to χ = 0, the OD stretch peak position shifted by $<$1 cm^{-1}. As mentioned above such a small shift would be difficult to observe in the overlapping spectra of free phenol and the complex shown in Fig. 1*a*. The mixtures observed here are ternary, that is, a solute, phenol, in a binary mixture of mesitylene and CCl_4. This is in contrast to a binary mixture in which the IR spectrum of one of the components is studied. In a study of the binary mixture $CH_3I/CHCl_3$, in which the absorption spectra of a CH stretch of CH_3I were studied, a 10 cm^{-1} spectral shift was observed in going from pure CH_3I to dilute CH_3I (12). The insignificant spectral shift observed here compared with the larger one observed in the binary mixture might be understood qualitatively in terms of the differences in the dielectric constants. Mesitylene and CCl_4 have dielectric constants of 2.3 and 2.2, respectively, an almost negligible difference. For CH_3I and $CHCl_3$, the dielectric constants are 7.0 and 4.8, respectively, indicating a larger change in local solvent properties as the mole fraction is varied.

To test whether the apparent preferential solvation of the phenol-mesitylene complex by mesitylene is caused by some feature of the mixed solvent itself, IR absorption spectra of mesitylene without the phenol solute were measured as a function of mole fraction in the mixed solvent. Mesitylene has an absorption band at $\approx$2,730 cm^{-1} (Fig. 1*c*) that is well separated from other peaks. Spectra for two of the mole fractions are shown in Fig. 1*e* (χ = 0.17 and χ = 1, lower and higher frequency peaks, respectively). The line width of this band as a function of χ is plotted in Fig. 1*b* (circles, right axis). The dashed line is the best linear fit to the data. The mesitylene line width increases linearly with increasing χ. These results suggest that mesitylene and CCl_4 maintain a homogeneous mixture as the mole fraction increases. Note that the shift in peak position for the two peaks shown in Fig. 1*c* is only 1 cm^{-1}.

The 2D-IR vibrational echo data presented in the next section provides detailed information on dynamics of the first solvation shell and differences in the dynamics in the mixed and pure solvents. In addition, the results provide some further indications of preferential solvation.

2D-IR Vibrational Echo Spectroscopy. As discussed briefly in *Materials and Methods*, 2D vibrational echo spectra are obtained for a range of values of T_w, the time between the second and third pulses in the vibrational echo sequence. As T_w increases, structural evolution of the solvent–solute system causes the shape of the 2D spectrum to change. The changes are caused by the coupling of the solvent structure to the hydroxyl stretch transition frequency of the phenol. The evolution of the spectrum is

referred to as spectral diffusion. Besides the T_w-dependent contributions to the 2D spectrum, there are T_w-independent contributions. There are three contributions to the line shapes that are T_w independent. The major contribution is produced by very fast structural fluctuations that generate a motionally narrowed component. There are also small contributions from the vibrational population relaxation (vibrational lifetime) and orientational relaxation. If there were only the fast motionally narrowed fluctuations and the vibrational and orientational relaxations, the linear absorption spectrum would be a perfect Lorentzian line shape, and the vibrational echo spectrum would have the corresponding 2D shape. Inhomogeneous broadening at short time modifies the 2D vibrational echo spectrum and also changes the shapes of the linear absorption spectra. Inhomogeneous broadening in the 2D spectrum is eliminated by spectral diffusion at long time. The shape of the 2D spectrum changes as spectral diffusion proceeds.

T_w-dependent vibrational echo spectra are obtained for four species, phenol in pure CCl_4, phenol in pure mesitylene, and phenol in the mixed mesitylene-CCl_4 solvent. In the pure solvents, there is a single phenol species, free phenol in pure CCl_4 and the phenol-mesitylene complex in pure mesitylene. These have the OD hydroxyl stretch absorption spectra very similar to the high frequency and low frequency peaks in Fig. 1*a*, respectively. As discussed in connection with Fig. 1, the mixed solvent has both species in equilibrium. In the 2D-IR vibrational echo experiment there are quantum pathways that involve only the $v = 0$ to $v = 1$ vibrational transition. There are also pathways that involve first the 0–1 transition (first two matter–radiation field interactions) and then the 1–2 transition (third interaction and vibrational echo emission). The pathways that include the 1–2 transition produce an off-diagonal peak shifted to lower frequency along the echo emission frequency axis (ω_m axis, see below) for each diagonal peak. For the OD hydroxyl stretch, the 1–2 off-diagonal bands are well separated from the 0–1 diagonal bands. In a comparative study of the bands for the system phenol in the mixed solvent benzene-CCl_4, which displays both free phenol and the phenol-benzene complex, the dynamical evolution of the 0–1 and 1–2 sets of bands were identical (8, 9). Therefore, we will only discuss the 0–1 bands here. Then, the single species samples give rise to a single diagonal peak, and the mixed solvent sample has two peaks on the diagonal. For the mixed solvent, chemical exchange between the phenol-mesitylene complex and free phenol will cause off-diagonal peaks to grow in. However, chemical exchange for this system occurs on a sufficiently long time scale (10) to be unimportant for the determination of spectral diffusion, which is of interest here.

As discussed in detail below, all four peaks have a sizable motionally narrowed component. For phenol in CCl_4, the absorption line shape can be fit to a perfect Lorentzian. Nonetheless, all of the species are inhomogeneously broadened to some extent and display spectral diffusion. As an example, the top panels in Fig. 2 show the 2D spectra for the phenol OD stretch in CCl_4 at very short (0.2 ps) and long (10 ps) T_ws. The ω_τ axis is the axis of the first matter-radiation field interaction. This axis is obtained by Fourier transformation of the interferograms recorded when the time, τ, between the first and second pulses in the echo pulse sequence is scanned. The ω_m axis is the axis of the third interaction and vibrational echo emission. The vibrational echo is heterodyned with a local oscillator pulse and passed through a monochromator and spectrally resolved. The resolution of the heterodyned pulse into its frequency components by the monochromator is the second Fourier transform. The procedure used virtually eliminates the dispersive contribution, and the spectra are essentially absorptive (13, 14). At 0.2 ps, the 2D spectrum is elongated along the diagonal, which is the signature of inhomogeneous broadening. By 10 ps, the spectrum

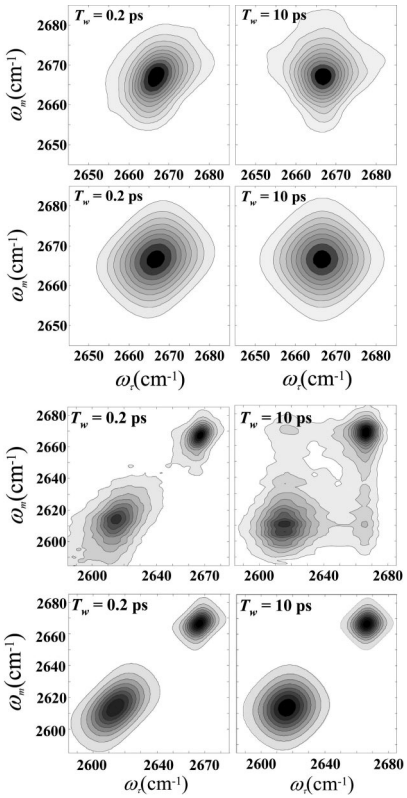

Fig. 2. 2D-IR spectra. (*Top*) 2D-IR vibrational echo data for phenol-OD in pure CCl_4 at two values of T_w. At short time the spectrum shows inhomogeneous broadening by the elongation along the diagonal. At long time, the spectrum shows that the system is dynamically broadened (all solvent structures sampled) by the symmetrical shape. (*Upper Middle*) The corresponding calculated spectra obtained from the frequency-frequency correlation function found by simultaneous fitting of the 2D spectra at 14 T_ws and the linear absorption spectrum. (*Lower Middle*) 2D-IR vibrational echo spectra data taken on the mixed solvent. The two peaks correspond to the two peaks in the absorption spectrum shown in Fig. 1*a*. At $T_w = 200$ fs, both peaks are elongated along the diagonal, but by 10 ps they have become much more symmetrical. At 10 ps, off-diagonal peaks arising from chemical exchange are just beginning to appear. (*Bottom*) The corresponding calculated 2D spectra. Because exchange was not included in the calculations, the off-diagonal peaks are not present in the 10-ps panel.

is symmetrical and has the characteristic diamond-like shape associated with a band that has a major motionally narrowed contribution. The symmetrical shape occurs when the spectrum is fully dynamically broadened, that is, the initial inhomogeneous distribution of frequencies has been randomized because all of the solvent structures have been sampled.

To obtain detailed information from the 2D-IR spectra, quantification of the line shape change with T_w is required. The experimental observables and the underlying dynamics can be related through the frequency–frequency correlation function (FFCF) (15, 16). The FFCF provides information on the amplitudes and time scales of OD stretch vibrational frequency fluctuations that are caused by solvent structural evolution. Global fitting was performed to derive the FFCF for each of the four bands (one in each pure solvent and two in the mixed solvent). For a particular peak, the FFCF, $C(t)$, was varied to simultaneously fit the linear IR spectrum and 14 T_w-dependent 2D-IR spectra. Various forms of the FFCF were considered, but it was sufficient to use a biexponential function

$$C(t) = \Delta_0^2 \exp(-t/\tau_0) + \Delta_1^2 \exp(-t/\tau_1) \qquad [1]$$

Table 1. Vibrational lifetimes (T_1), orientational relaxation time constants (τ_r), and Lorentzian contribution to the line width from the two relaxation processes for the four species

Species (solvent)	T_1, ps	τ_1, ps	Line width, cm^{-1}
Free (CCl_4)	12.5 ± 0.5	2.9 ± 0.5	1.6
Free (mixed)	12.5 ± 1	2.9 ± 0.5*	1.6
Complex (mes.)	7.6 ± 0.5	5.5 ± 0.5	1.3
Complex (mixed)	7.6 ± 1	4.5 ± 0.5*	1.5

*The rotational relaxation time corrected for the changes in viscosity from the pure solvents where they were measured.

to calculate the linear and third order response functions necessary to obtain the linear and 2D spectra. The τ_i set the time scale of the dynamics and the corresponding Δ determines the amplitude. To establish the FFCF for a particular peak, the calculated line shapes are iteratively compared with the experimental data until convergence. The vibrational lifetime and orientational relaxation rate are included in the calculations. The lifetimes and orientational relaxation rates were measured by using polarized IR pump-probe experiments. These values are presented in Table 1. In addition, the total Lorentzian contribution to the absorption line width from these two processes is given in Table 1. In the fitting, the lifetimes and orientational relaxation rates were varied 15%. This variation made no difference in the fits because the contribution to the linear and 2D spectra from these processes is small.

From the results of fitting the linear and 2D spectra for each of the species, it was found that all of the FFCFs have one component of Eq. **1** that is motionally narrowed. Motional narrowing occurs when $\Delta\tau < 1$. For the motionally narrowed component, Δ and τ cannot be independently determined. Only $\Gamma^* = \Delta^2\tau/\pi$ can be obtained from the fits to the data. Γ^* is the motionally narrowed line width. Γ^* gives a Lorentzian contribution to the linear absorption spectrum, and it makes a T_w-independent contribution to the 2D spectrum.

Fig. 2 *Upper Middle* shows two calculated 2D spectra for free phenol in CCl_4 that correspond to the two experimental spectra of the 14 measured spectra that are displayed in Fig. 2 *Top*. Fig. 2 *Lower Middle* show data taken on the mixed solvent. The two peaks correspond to the two peaks in the absorption spectrum shown in Fig. 1*a*. At $T_w = 200$ fs, both peaks are elongated along the diagonal, but by 10 ps they have become much more symmetrical. At 10 ps, off-diagonal peaks arising from chemical exchange are just beginning to appear (8, 9, 17). Because the exchange rate is very slow, exchange does not need to be included in the calculation of the spectral diffusion (9). Fig. 2 *Bottom* shows the corresponding calculated 2D spectra. Because exchange was not included in the calculations, the off-diagonal peaks are not present in the 10 ps panel. The method for performing the calculations of spectral diffusion with exchange has been presented (9). The FFCF parameters are given in Table 2 for free phenol in pure CCl_4, free phenol in the mixed mesitylene/CCl_4 solvent, the phenol-mesitylene complex in pure mesitylene, and the complex in the mixed solvent. The line width of the motionally narrowed component of the FFCF is given in column 1, and the amplitude and time constant of the other component are given in columns 2 and 3, respectively.

Table 2. FFCF parameters for the four species

Species (solvent)	Γ^*, cm^{-1}	Δ_1, cm^{-1}	τ_1, ps
Free (CCl_4)	10.2 ± 0.5	2.9 ± 0.5	5 ± 0.5
Free (mixed)	10.3 ± 0.5	3.0 ± 0.5	13 ± 1
Complex (mes.)	22 ± 1	6.5 ± 0.5	10 ± 1
Complex (mixed)	21 ± 1	6.7 ± 0.5	24 ± 1

Looking at the parameters in Table 2, it is seen that the motionally narrowed components for the free species in pure CCl_4 and in the mixed solvent are identical. Furthermore, the motionally narrowed components for the complex in pure mesitylene and in the mixed solvent are identical, but significantly different from those of the free species. The motionally narrowed component of the free phenol peak in pure CCl_4 should arise from "collisions" between the solvent and the solute, that is, very fast small fluctuations of the solvent molecular positions in the first solvent shell of the solute (18).

The phenol mesitylene T-shaped complex is formed by a π hydrogen bond between the phenol hydroxyl and the mesitylene π system (4, 8, 10). The hydrogen bond shifts the hydroxyl stretch frequency to lower frequency (19). That the frequency shift is caused by hydrogen bonding in pure mesitylene and in the mixed solvent is demonstrated by the spectra of 2-methoxy phenol-OD in the two pure solvents, which does not hydrogen bond as discussed above. The 2-methoxy phenol OD stretch frequencies in CCl_4 and in mesitylene are 2,627 cm^{-1} and 2,626 cm^{-1}, respectively. The negligible change in frequency with the change in solvent demonstrates that the large shift in the phenol OD stretch frequency is not caused by a general solvent effect but rather by the specific hydrogen bonding of the phenol hydroxyl group to the mesitylene.

The phenol-mesitylene hydrogen bond also provides a mechanism for the fast motionally narrowed vibrational dephasing. The motionally narrowed line width, Γ^*, of the complex is a factor of two greater than that of the free species (see Table 2). For water, it has been demonstrated that a large motionally narrowed component of the FFCF is caused by local hydrogen bond fluctuations (20, 21). The motionally narrowed component dominates the FFCF in water with smaller slower contributions coming from global structural rearrangements of the liquid. In pure mesitylene, the solvent shell surrounding the complex is composed of mesitylene molecules. The mixed solvent sample is 83% mol/mol CCl_4. Therefore, in the mixed solvent there are slightly more than four CCl_4 molecules per mesitylene. If the first solvent shell of the complex in the mixed solvent had the stoichiometric ratio, then its composition would be predominantly CCl_4, and it would be quite different from that of the complex in pure mesitylene. In both solvents, the motionally component would be caused by complex's hydrogen bond geometry fluctuations. It is possible that the nature of the local solvent plays no role in the fast fluctuations of the structure of the complex. However, in going from a pure mesitylene solvent to one that is 83% CCl_4, it might be expected that there would be some differences in the rates or amplitudes. The fact that the motionally narrowed components for the complexes in the two solvents are identical within experimental error (see Table 2) suggests preferential solvation of the complex by mesitylene in the mixed solvent. The first solvent shell of the complex might be predominantly but not exclusively mesitylene (see below).

The results presented in Fig. 1*b* along with the values of the Γ^* for the free and complexed species in the pure and mixed solvents provide some evidence for preferential solvation in the mixed solvent. Preferential solvation is also supported by related MD simulations on the system of phenol in the benzene/CCl_4 mixed solvent (4). These very detailed simulations show that the solvent shells around the phenol-benzene complex and free phenol do not have the stoichiometric ratio. However, consideration of the slow time scale components of the FFCFs (see Table 2) demonstrates that the complex and free phenol dynamics differ in the mixed and pure solvents. The slow components provide important information on the nature of the structural evolution of the first solvent shell.

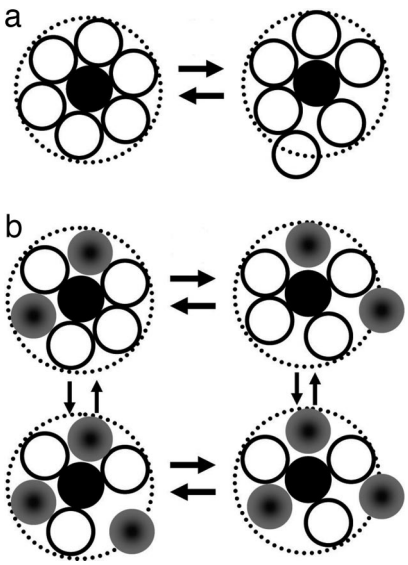

Fig. 3. Schematic illustrations of the mechanism for the slow component of the vibrational dephasing. (*a*) Pure solvent: density variations caused by diffusive first solvent shell structural fluctuations. (*b*) Mixed solvent: diffusive density and compositional fluctuations in the first solvent shell.

The FFCF amplitudes of the two species are independent of the solvent. The free phenol in pure CCl_4 has the identical amplitude (Δ_1) as free phenol in the mixed solvent (see Table 2). The Δ_1 for the complex in pure mesitylene is identical to that found for the mixed solvent. However, the dephasing time constants, τ_1, are all different. Although different, there is a common feature to the τ_1 values. In each case, the species in the mixed solvent is $\approx$2.5 times slower than the same species in the pure solvent. These results can be understood in terms of a solvent diffusion model of the slow component of the FFCF.

Diffusive motion of solvent molecules in the first solvent shell can change the dispersion interaction between the solute and the solvent (18). As a result, changes in the attractive part of the solute-solvent potential due to slow diffusion (slow compared with the essentially inertial fluctuations responsible for the motionally narrowed term) will generate the slow component of the vibrational frequency fluctuations. This model was applied to lineshapes of isotropic Raman spectra (18). In the context of the current experiments, it would predict the correlation decay time for the slow fluctuations, τ_1, to be

$$\tau_1 \approx \sigma^2/\pi^2 D, \qquad [2]$$

where D and σ are the solvent diffusion constant and molecular diameter, respectively. Eq. **2** would be appropriate for the pure solvents systems, free phenol in pure CCl_4 and the complex in pure mesitylene. The diffusion constants were obtained by using the Stokes–Einstein equation, $D = k_BT/3\pi\eta\sigma$, where η is the viscosity, T is the absolute temperature, and k_B is Boltzmann's constant (22). The calculated values are 3.2 ps for free phenol in CCl_4 and 8 ps for the complex in mesitylene. These values agree remarkably well with the corresponding values of 5 and 10 ps extracted from the 2D-IR vibrational echo experiments. The agreement with the calculations supports but does not prove the proposition that the mechanism giving rise to the slow component of the FFCF is time-dependent density variations caused by diffusive motion of the solvent in the first solvation shell. A schematic illustration of this mechanism is shown in Fig. 3*a*. At a given instant, the solutes experience a distribution of local solvent densities in the first solvent shell. The distribution of local solvent densities produces inhomogeneous broadening of the OD stretch in the absorption spectrum and in the 2D vibrational echo spectrum at short T_w. The time required to randomize the initial distribution of local densities is determined by the diffusion constant. As shown in Fig. 2, when T_w is increased, the system goes from being inhomogeneous (elongation along the diagonal) to fully dynamically broadened (symmetric shape).

The same type of mechanism can be used to explain the significantly slower time scale of the dephasing in the mixed solvents compared with the free solvents, that is, the longer τ_1 values. In the mixed solvent, in addition to density variations, there will also be compositional variations in the first solvent shell. Even if there is preferential solvation, the composition of the first solvation shells will not be identical for all solutes. This is illustrated schematically in Fig. 3*b*. As mentioned above, recent MD simulations provide insights into the solvation structure of a system very similar to the one studied here (4). The MD simulations addressed the system phenol in the mixed solvent benzene/CCl_4. The results showed that both free phenol and the phenol-benzene complex are preferentially solvated but there are discretely different first solvent shell compositions at a given time which are distinct from the stoichiometric composition of the mixed solvent; there is local inhomogeneity of the solvation structure in the mixed system.

Compositional variation in the first solvent shell of the solutes in the mixed solvent gives rise to the increase in the τ_1 values. As illustrated in Fig. 3*b*, to go from inhomogeneous broadening at short T_w to completely dynamically broadened at long T_w, the mixed solvent system must randomize both the density variations and the compositional variations. The relaxation of both types of processes will occur on a time scale determined by molecular diffusion. However, the addition of the compositional variations in the first solvent shell requires the system to have different species move into and out of the first solvent shell rather than simply relaxing configurational variations that occur in the pure solvent.

Concluding Remarks

The solute–solvent structure and dynamics in the mixed solvent mesitylene/CCl_4 as well as in the pure solvents mesitylene and CCl_4 were studied for two types of solutes, free phenol (uncomplexed) and the phenol-mesitylene T-shaped complex. Free phenol exists in pure CCl_4 and in the mixed solvent. The complex exists in pure mesitylene and in the mixed solvent. In the mixed solvent, the complex and free phenol are in equilibrium with a complex dissociation time constant of 31 ps (10).

The 2D-IR experiments explored vibrational dephasing of the hydroxyl stretch of phenol for free phenol in CCl_4 and in the mixed solvent, and the complex in mesitylene and in the mixed solvent. All four systems have motionally narrowed components in the 2D spectra. In addition, each system has a slower time scale component of the vibrational dephasing. For the solutes in the pure solvents, the observed slow dephasing times were described in terms of a model involving diffusive density fluctuations in the solute's first solvent shell (18). This model almost reproduced the observed dephasing times quantitatively. In the mixed solvents, the slow component of the vibrational dephasing lengthened by a factor of $\approx$2.5. The increased dephasing time is attributed to compositional variations in the first solvent shells of the solutes. In the mixed solvent, the variations in composition in addition to the density variations need to randomize, which increases the time required for the system to sample all configurations.

The phenol-mesitylene system was chosen for study because the chemical exchange time constant between complex and free phenol is 31 ps, compared with, e.g., 10 ps for phenol-benzene (8–10). The phenol-mesitylene complex-free exchange rate is sufficiently long that the spectral diffusion can be measured without a significant contribution to the diagonal peaks' line

broadening from chemical exchange. Exchange influences the diagonal line shape when the there is an even number of steps, that is, a dissociation followed by reformation of the complex, or formation followed by dissociation (9). The time scale for the two steps is substantially longer than the spectral diffusion time. Nonetheless, these results bring out an interesting aspect of spectral diffusion in the system that is exchanging that will be important for systems that exchange faster than the time scale for the relaxation of compositional fluctuations. The exchanging species can have different compositions in the first solvent shell that might influence the exchange rate. Therefore, depending the on the time scale of chemical exchange vs. that of composition randomization, the exchange rate might not be a single value but rather a compositionally inhomogeneous distribution of rates.

Materials and Methods

Materials and Sample Preparation. All chemicals were purchased from Sigma–Aldrich (St. Louis, MO) and used as received. The deuterated hydroxyl hydrogen (OD) of the phenol was prepared by deuterium exchange with methanol OD. The procedure for deuteration has been detailed (23).

2D-IR Vibrational Echo Spectroscopy. The 2D-IR vibrational echo spectrometer is similar to an experimental setup described in ref. 14. Three transform limited (60 fs, 250 cm^{-1} FWHM) mid-IR laser pulses are sequentially time delayed before they are brought into the sample. The vibrational echo pulse generated in the sample is emitted in the phase-matched direction, made colinear with a local oscillator pulse, and dispersed through a monochromator onto a two-dimensional 2×32-element MCT array detector. The top 32 elements receive the signal mixed with the local oscillator, and the bottom 32 elements receive only the local oscillator. The signal from the bottom array was used for correcting frequency dependent laser fluctuations. The signal is mixed with the local oscillator to obtain full time, frequency, and phase information about the vibrational echo wave packet. The laser frequency was tuned to coincide with the maximum of the absorption frequency for each sample. For studies on pure CCl_4 and mesitylene, the laser frequency was set at 2,666 and 2,614 cm^{-1}. For the mixture, it was tuned between the two absorption bands, 2,640 cm^{-1}. In all samples, the broadband laser pulse afforded sufficient bandwidth to observe both 0–1 and 1–2 vibrational transitions. To avoid broadening due to truncation of signal, interferograms were obtained to 4.5 ps.

For each sample, a family of vibrational echo 2D spectra is obtained as a function of three variables: the emitted vibrational echo frequencies, ω_m, and the variable time delays between the first and second pulses (τ) and the second and third pulses (T_w, "waiting" time). Frequency correlation maps are created by numerically Fourier transforming the τ scan data as a function of the emission frequencies, ω_m, at each T_w. Absorptive 2D-IR spectra are created via the dual-scan method (13, 14). The amplitude of the 2D-IR data at each fixed T_w is plotted as a function of the Fourier transformed τ decay, ω_τ (horizontal axis in the 2D plots), and emission frequency, ω_m (vertical axis in the 2D plots).

This work was supported by Air Force Office of Scientific Research Grant F49620-01-1-0018 and National Science Foundation Grant DMR-0332692.

1. Reichardt C (2003) *Slovents and Solvent Effects in Organic Chemistry* (Wiley-VCH, Berlin).
2. Gardecki JA, Maroncelli M (1999) *Chem Phys Lett* 301:571–578.
3. Marcus Y (2002) *Solvent Mixture* (Dekker, New York).
4. Kwac K, Lee C, Jung Y, Han J, Kwak K, Zheng J, Fayer MD, Cho M (2006) *J Chem Phys* 125:244508.
5. Suppan P (1997) *Solvatochromism* (R Soc Japan, Tokyo).
6. Bangno A, Scorrano G, Sitz S (1997) *J Am Chem Soc* 119:2299–2300.
7. Berg M, Vanden Bout DA (1997) *Acc Chem Res* 30:65–71.
8. Zheng J, Kwak K, Asbury JB, Chen X, Piletic I, Fayer MD (2005) *Science* 309:1338–1343.
9. Kwak K, Zheng J, Cang H, Fayer MD (2006) *J Phys Chem B* 110:19998–20013.
10. Zheng J, Fayer MD (2006) *J Am Chem Soc*, in press.
11. Kim YS, Hochstrasser RM (2005) *Proc Natl Acad Sci* 102:11185–11190.
12. Knapp EW, Fischer SF (1982) *J Chem Phys* 76:4730–4735.
13. Khalil M, Demirdoven N, Tokmakoff A (2003) *Phys Rev Lett* 90:047401.
14. Asbury JB, Steinel T, Fayer MD (2004) *J Lumin* 107:271–286.
15. Mukamel S (2000) *Annu Rev Phys Chem* 51:691–729.
16. Mukamel S (1995) *Principles of Nonlinear Optical Spectroscopy* (Oxford Univ Press, New York).
17. Zheng J, Fayer MD (2007) *J Am Chem Soc* 129:4328–4335.
18. Schweizer KS, Chandler D (1982) *J Chem Phys* 76:2296–2314.
19. Pimentel GC, McClellan AL (1960) *The Hydrogen Bond* (Freeman, San Francisco).
20. Fecko CJ, Loparo JJ, Roberts ST, Tokmakoff A (2005) *J Chem Phys* 122:054506.
21. Asbury JB, Steinel T, Kwak K, Corcelli S, Lawrence CP, Skinner JL, Fayer MD (2004) *J Chem Phys* 121:12431–12446.
22. Berry RS, Rice SA, Ross J (2000) *Physical Chemistry* (Oxford Univ Press, New York).
23. Zheng J, Kwak K, Chen X, Asbury JB, Fayer MD (2006) *J Am Chem Soc* 128:2977–2987.